J Ginseng Res 44 (2020) 258–266

Contents lists available at ScienceDirect

Journal of Ginseng Research

journal homepage: http://www.ginsengres.org

Research Article

The role of ginsenoside Rb1, a potential natural glutathione reductase agonist, in preventing oxidative stress-induced apoptosis of H9C2 cells

Hui-Jie Fan [1,5,☆], Zhang-Bin Tan [1,☆], Yu-Ting Wu [1,☆], Xiao-Reng Feng [3,☆], Yi-Ming Bi [1], Ling-Peng Xie [1], Wen-Tong Zhang [1], Zhi Ming [1], Bin Liu [4,**], Ying-Chun Zhou [1,2,*]

[1] School of Traditional Chinese Medicine, Southern Medical University, Guangzhou, China
[2] Department of Traditional Chinese Medicine, Nanfang Hospital, Southern Medical University, Guangzhou, China
[3] Department of Orthopaedics and Traumatology, Queen Mary Hospital, the University of Hong Kong, Hong Kong
[4] Department of Cardiology, The Second Affiliated Hospital of Guangzhou Medical University, Guangzhou, China
[5] Department of Traditional Chinese Medicine, The first hospital of Yangjiang, Yangjiang, China

ARTICLE INFO

Article history:
Received 24 February 2018
Received in Revised form
27 November 2018
Accepted 10 December 2018
Available online 16 December 2018

Keywords:
Apoptosis
Ginsenoside Rb1
Glutathione reductase
H9C2
Oxidative stress

ABSTRACT

Background: Oxidative stress-induced cardiomyocytes apoptosis is a key pathological process in ischemic heart disease. Glutathione reductase (GR) reduces glutathione disulfide to glutathione (GSH) to alleviate oxidative stress. Ginsenoside Rb1 (GRb1) prevents the apoptosis of cardiomyocytes; however, the role of GR in this process is unclear. Therefore, the effects of GRb1 on GR were investigated in this study.

Methods: The antiapoptotic effects of GRb1 were evaluated in H9C2 cells by 3-(4,5-dimethylthiazol-2-yl)-2,5-diphenyltetrazolium bromide, annexin V/propidium iodide staining, and Western blotting. The antioxidative effects were measured by a reactive oxygen species assay, and GSH levels and GR activity were examined in the presence and absence of the GR inhibitor 1,3-bis-(2-chloroethyl)-1-nitrosourea. Molecular docking and molecular dynamics simulations were used to investigate the binding of GRb1 to GR. The direct influence of GRb1 on GR was confirmed by recombinant human GR protein.

Results: GRb1 pretreatment caused dose-dependent inhibition of tert-butyl hydroperoxide-induced cell apoptosis, at a level comparable to that of the positive control N-acetyl-L-cysteine. The binding energy between GRb1 and GR was positive (−6.426 kcal/mol), and the binding was stable. GRb1 significantly reduced reactive oxygen species production and increased GSH level and GR activity without altering GR protein expression in H9C2 cells. Moreover, GRb1 enhanced the recombinant human GR protein activity *in vitro*, with a half-maximal effective concentration of ≈2.317 μM. Conversely, 1,3-bis-(2-chloroethyl)-1-nitrosourea co-treatment significantly abolished the GRb1's apoptotic and antioxidative effects of GRb1 in H9C2 cells.

Conclusion: GRb1 is a potential natural GR agonist that protects against oxidative stress–induced apoptosis of H9C2 cells.

1. Introduction

Cardiovascular diseases (CVDs) are one of the leading causes of morbidity and mortality worldwide. Oxidative stress, which may cause apoptosis of myocardial cells, is widely targeted as an important pathogenic mechanism involved in atherosclerosis, myocardial infarction, ischemic heart disease, reperfusion injury, and heart failure [1,2]. It has been reported that the inhibition of excessive oxidative stress and cardiac muscle cell apoptosis are promising approaches to the protection of cardiomyocytes and management of CVDs [3–5].

Glutathione (GSH) is formed from glutamate, cysteine, and glycine [6]. As a crucial antioxidant, GSH exhibits antiinflammatory [7], antiproliferative [8], and antiapoptotic effects [9] and helps to

* Corresponding author. School of Traditional Chinese Medicine, Southern Medical University, 1063 Shatai Road, Guangzhou, Guangdong, 510515, China.
** Corresponding author. Department of Cardiology, The Second Affiliated Hospital of Guangzhou Medical University, Guangzhou, Guangdong, 510260, China.
E-mail addresses: xmhoolv@163.com (B. Liu), zhychun@126.com (Y.-C. Zhou).
☆ These authors contributed equally.

https://doi.org/10.1016/j.jgr.2018.12.004
p1226-8453 e2093-4947/$ – see front matter

maintain cellular homeostasis [10]. GSH protects cells from oxidative stress by a decrease in the intracellular level of reactive oxygen species (ROS) [11], and it is formed by the reduction of glutathione disulfide (GSSG) by the key enzyme glutathione reductase (GR), which increases the GSH/GSSG ratio [12]. Maintaining a high GSH/GSSG ratio helps balance cellular redox signaling and diminishes thiol oxidative stress [13]. Hence, GR agonists might provide strong protective effects against oxidative stress-related diseases. However, information on GR agonists is lacking.

Many traditional Chinese medicines have been investigated in clinical studies. Our target compound, ginsenoside Rb1 (GRb1), is a significant active constituent, primarily found in ginseng, pseudo ginseng, and American ginseng. An extract prepared from the latter has been shown to protect the heart from ischemia and reperfusion injury by upregulating the expression of endothelial nitric oxide synthase [14]. In addition, GRb1 has been reported to have diverse pharmacological functions, such as improving cardiac function and remodeling in heart failure, protecting against ischemia/reperfusion-induced myocardial injury, alleviating osteoblast dysfunction and fatty liver, and improving insulin resistance [15–19]. Moreover, the antioxidative properties of GRb1 allow it to scavenge free oxygen radicals to prevent oxidative stress–induced cell apoptosis [20].

Little is known, however, about the effect of GRb1 on GR activity; therefore, our study was designed to investigate whether GRb1 is a GR agonist or an enzyme inducer, and whether it protects cardiomyocytes from oxidative stress–induced apoptosis by increasing GR activity.

2. Material and methods

2.1. Chemicals and reagents

GRb1 (purity>98%) was purchased from Chengdu Must Bio-Technology Co., Ltd. (Chengdu, China), and a GR recombinant protein (purity>95%) was purchased from Thermo Fisher Scientific (Rockford, IL, USA). The GR inhibitor carmustine [1,3-*bis*-(2-chloroethyl)-1-nitrosourea(BCNU); purity>98%] was purchased from Sigma–Aldrich (St. Louis, MO, USA). Tert-butyl hydroperoxide (TBHP) was purchased from Sigma (St. Louis, MO, USA). Antibodies against glyceraldehyde 3-phosphate dehydrogenase (GAPDH), B-cell lymphoma 2 (BCL-2), and BCL-2-associated X protein (BAX) were purchased from Cell Signaling Technology (Danvers, MA, USA). GR antibody was purchased from Abcam (Cambridge, MA, USA). GSH and lactate dehydrogenase (LDH) assay kits were purchased from Nanjing Jiancheng Bioengineering Institute (Nanjing, China). *N*-acetyl-L-cysteine (NAC), GR activity kit, and ROS assay kit were purchased from Beyotime Biotechnology (Shanghai, China). An annexin V/propidium iodide (PI) apoptosis detection kit was purchased from BD Bioscience (San Jose, CA, USA). The other reagents used in this study were obtained from commercial sources.

2.2. Cell culture

H9C2 cells, derived from embryonic rat heart cells, were obtained from the Cell Bank of the Type Culture Collection of the Chinese Academy of Sciences (Shanghai, China) and maintained in Dulbecco's modified Eagle's medium supplemented with 10% fetal bovine serum, 100 U/mL penicillin, and 100 μg/mL streptomycin at 37°C in a humidified atmosphere containing 5% CO_2.

2.3. Cell viability assay

H9C2 cells were plated at a density of 5.0×10^3 cells per well in 96-well plates. After 2 h of incubation with or without the GR inhibitor BCNU, the cells were treated for 24 h with GRb1 (25, 50, or 100 μM) or 1 mM NAC, followed by incubation with or without 150 μM TBHP for 2h. Cell viability was determined by 3-(4,5-dimethylthiazol-2-yl)-2,5-diphenyltetrazolium bromide (MTT) assay as described previously [13]. Briefly, the culture medium was removed and replaced with an MTT solution (0.5 mg/mL) for 4 h at 37°C, and then the MTT solution was replaced with 150 μL of dimethyl sulfoxide (Sigma–Aldrich) to dissolve the formazan crystals formed. The amount of formazan was quantified by measuring absorbance at 490 nm using a microplate reader (BioTek Instruments, Winooski, VT, USA). Cell viability was calculated as a percentage relative to that in the control group.

2.4. Detection of apoptosis by annexin V/PI staining

H9C2 cells were seeded into a 96-well plate and treated with NAC or GRb1, followed by incubation with or without 50 μM BCNU for 2 h before treatment with 1 mM NAC or GRb1 (25, 50, or 100 μM) for 24 h. The cells were then treated with 150 μM TBHP for 2 h, except in the control group. The apoptosis index of H9C2 cells was determined using a fluorescein isothiocyanate-labeled annexin V/PI apoptosis kit (BD Biosciences) according to the manufacturer's instructions, and the cells undergoing apoptosis were then quantified by averaging cell counts in three or four randomly selected fields per plate. The ratio of both types of stained cells to the total nuclei was calculated to evaluate the percentage of apoptotic cells.

2.5. LDH release assay

During apoptosis, nicotinamide adenine dinucleotide (NAD^+) is reduced to NADH by LDH, which is then released into the cell culture medium from the cytoplasm, leading to cytomembrane damaged. Additionally, diaphorase catalyzes the reaction between 2-*p*-iodophenyl-3-nitrophenyl tetrazolium chloride and NADH to produce formazan, which has an absorption peak at 490 nm. Based on this reaction, LDH cytotoxicity assay kit was used to measure the absorbance of LDH after the different treatments. H9C2 cells were seeded into a 96-well plate and treated as described in Section 2.4. After treatment, the cell culture medium was collected, and LDH activity was measured using an LDH assay kit, according to the manufacturer's instructions. An LDH releasing agent was provided in the kit and served as the positive control of total LDH release. Absorbance was measured at 490 nm using a microplate reader (BioTek Instruments), and the LDH index was calculated as follows: LDH index= (OD mean test group/OD mean total LDH release group)/(OD mean control group/OD mean total LDH release group) × 100%.

2.6. GSH assay

H9C2 cells were treated as described above, and then cell lysates were prepared using a cell lysate buffer (Beyotime). The GSH levels in the cell lysates were determined using the GSH assay kit, following the manufacturer's protocol. Briefly, GSH was reacted with 5,5′-dithiobis (2-nitrobenzoic acid) to produce GSSG and 5′-thio-2-nitrobenzoic acid (TNB). The TNB absorbance was measured at 405nm, and the GSH content was calculated based on the TNB concentration. The final GSH content was expressed as micromoles per gram protein.

2.7. ROS detection

ROS concentrations were measured using 2′,7′-dichlorodihydrofluorescein diacetate (DCFH-DA). H9C2 cells were treated as described above and then washed three times with phosphate-

buffered saline, followed by the addition of 10 μM DCFH-DA and incubation at 37°C for 20 min. Afterward, DCFH-DA was removed, and the cells were washed again with phosphate-buffered saline three times. The fluorescence intensity was evaluated using flow cytometry.

2.8. Assessment of GR activity

In the present study, GR activity was calculated based on the decrease of NADPH levels, measured at 340 nm. The change in GR activity was measured in H9C2 cells grown with different treatments and after incubation of GR recombinant protein with different GRb1concentrations.

2.8.1. GR activity in H9C2 cells

H9C2 cell lysates were prepared as described above, and GR activity was determined using a GR activity kit according to the manufacturer's instructions. GR activity was expressed in milliunits per milligram protein.

2.8.2. GR activity of GRb1-pretreated GR recombinant protein

GRb1 at final concentrations of 0.097, 0.195, 0.039, 0.78, 1.56, 3.13, 6.25, 12.5, 25, and 50 μM was added to GR recombinant protein diluted with 0.02 M 1-piperazineethanesulfonic acid (pH 7.5). The samples were incubated at room temperature for 1 h. Afterward, GR activity was measured as described above. The half-maximal effective concentration (EC_{50}) and $\log_{10}$-transformed EC_{50} value of GRb1 were determined by nonlinear least-squares curve fitting (GraphPad Prism 5.0; GraphPad Software, Inc., La Jolla, CA, USA).

2.9. Western blot analysis

Western blot analysis was performed as described previously [14]. Proteins were extracted from H9C2 cells using a lysis buffer, and the lysates were centrifuged for 15 min at 4°C. Subsequently, 15 μg of protein from each sample was subjected to sodium dodecyl sulfate polyacrylamide gel electrophoresis and transferred onto a polyvinylidene difluoride membrane (Millipore, Bedford, MA, USA). The membrane was blocked with tris-buffered saline containing 5% nonfat milk, followed by incubation with target primary antibodies overnight at 4°C (GR, 1:1,000; BAX, 1:1,000, BCL-2, 1:1,000, and GAPDH 1:3,000). The intensity of each band was quantified using the Image J software and normalized to that of the loading control (GAPDH).

2.10. Molecular docking and molecular dynamics

Molecular docking was performed using AutoDock Vina (Scripps Research Institute, USA) to elucidate the binding mechanism between GR [Protein Data Bank (PDB) ID: 1GRE] and GRb1 [compound ID (CID):9898279]. The GR target protein was prepared for molecular docking simulations by removing water molecules and co-crystallized ligands. The flavin adenine dinucleotide–binding domain of GR was defined in this study as the ligand-binding site of GR, in which the energy of ligand binding to GR was used to evaluate the binding ability. PyMOL v.1.3 was used to visualize the results, and YASARA was used to minimize the ligand energy and perform molecular dynamics simulations. All simulations were run with the AMBER03 force field. The best conformations were regarded as the star conformations for molecular dynamics simulations. In particular, a 0.9% NaCl solution served as the solvent for the receptor–ligand complex in a dodecahedron box, with a distance of 5 Å between the box and the solute. The initiation of simulated annealing minimizations was set at 298K, with velocities scaled down by 0.9 every 10 steps, lasting for 5 ps. Following energy minimization, the temperature of the system was adjusted using a Berendsen thermostat to minimize the influence of temperature control. In addition, velocities were rescaled after every 100 simulation steps, whenever the mean of the last 100 detected temperatures converged. Finally, 100-ns molecular dynamics simulations were conducted at a rate of 2 fs, and the coordinates of the complexes were saved every 10 ps.

2.11. Data analysis

Data are expressed as the mean ± standard deviation (SD). One-way analysis of variance with least significant difference was performed for multiple comparisons. A Student *t*-test was used for statistical comparisons between treatment groups, with $p < 0.05$ considered significant. Calculations were performed using SPSS, 21.0(IBM Corporation, Armonk, NY, USA).

3. Results and discussion

3.1. GRb1 attenuates TBHP-induced apoptosis of H9C2 cells

As an organic peroxide, TBHP induces oxidative stress, which further leads to apoptosis [21,22]. The reducing agent NAC is a thiol-containing radical scavenger and GSH precursor [23]. Our results showed that TBHP triggered apoptosis of H9C2 cells compared with the control group; 150 μM TBHP decreased H9C2 viability to 50.17 ± 4.57% ($p < 0.01$), indicating that TBHP treatment could serve as a model group in researches on apoptosis *in vitro* (Fig. 1C). The protective effects of GRb1 against TBHP-induced apoptosis were examined by the annexin V/PI assay (Fig. 1A and B). The results indicated that GRb1 effectively decreased the apoptosis index. Moreover, the results of MTT assay showed that the viability of H9C2 cells was significantly reduced by TBHP treatment but was increased dose-dependently by GRb1 treatment (Fig. 1C). LDH is a well-known marker of cardiomyocyte injury; therefore, its release is closely related to the extent of cell membrane damage [24]. Our results (Fig. 1D) showed that GRb1 dose-dependently protected H9C2 cells from TBHP-induced LDH release.

The BCL-2 family of proteins includes antiapoptotic and proapoptotic proteins [25]. BAX is a major proapoptotic protein, whereas BCL-2 is a major antiapoptotic protein [26]. A high BAX/BCL-2 ratio would trigger apoptosis. Hence, we investigated whether GRb1 affects BCL-2 and BAX expression. Compared with their expression in the TBHP group, that of BCL-2 was enhanced, whereas BAX expression decreased in the GRb1-treated TBHP-induced apoptosis model (Fig. 1E and F). In previous reports, TBHP was found to trigger mitochondrial dysfunction, which led to an imbalance in the BAX/BCL-2 ratio [22,27]. Consistently, in our study, TBHP treatment significantly decreased BCL-2 expression, along with enhancement of BAX expression. Meanwhile, GRb1 remarkably counteracted the damage caused by TBHP in H9C2 cells, which indicated that GRb1 could serve as a cardioprotective agent. Based on the results obtained, GRb1 pretreatment successfully reduced the extent of apoptosis of H9C2 cells in the presence of TBHP.

3.2. Pretreatment with GRb1 reduces TBHP-induced oxidative stress in H9C2 cells

ROS play an important role in the oxidant system and can be generated by TBHP-treated H9C2 cells. Furthermore, ROS cause damage to the cell membrane and activate apoptotic pathways [28]. Therefore, the protective effect of GRb1 against TBHP-induced oxidative stress was initially examined by assaying ROS levels (Fig. 2A and B). Based on our results, TBHP could significantly

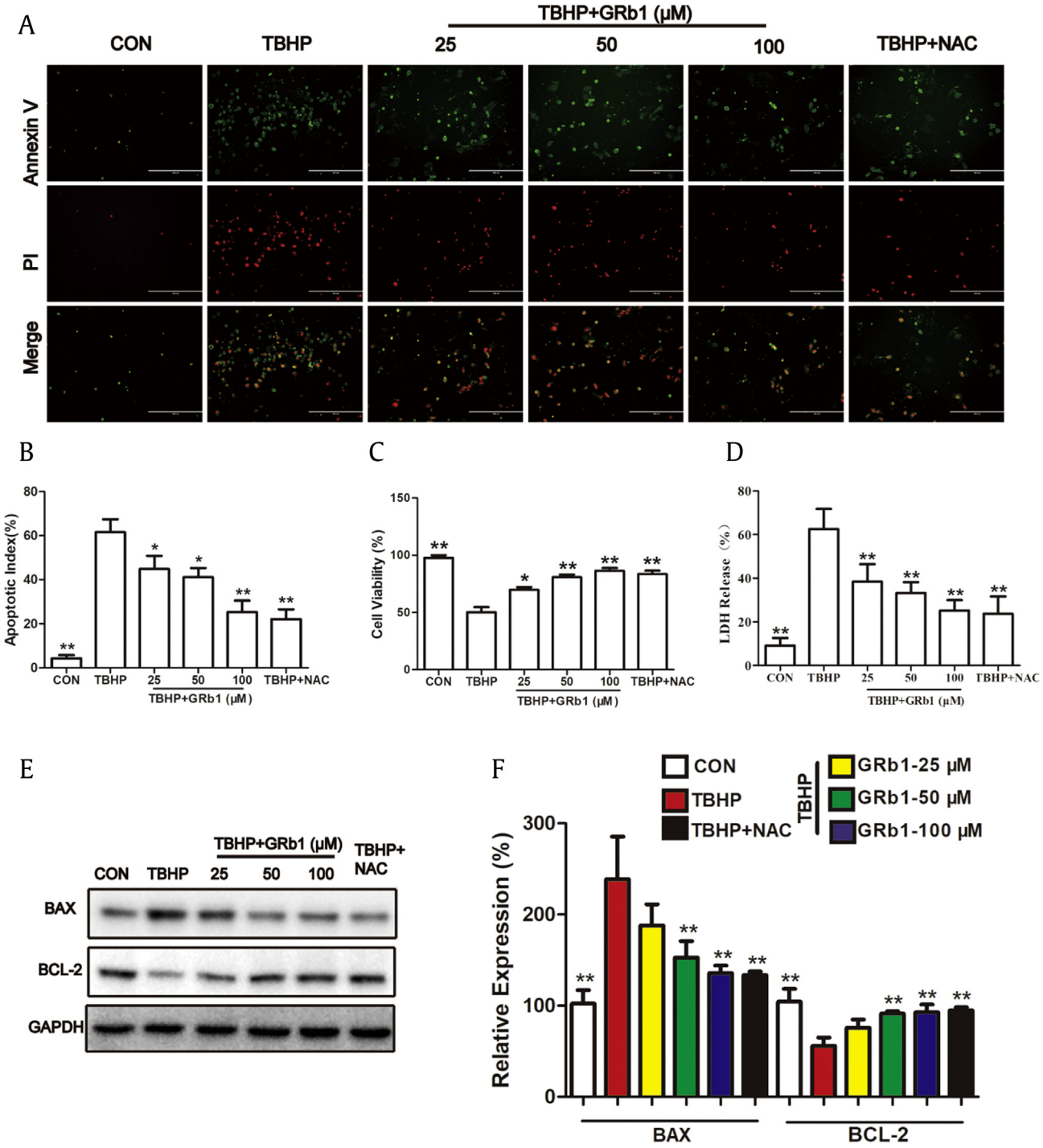

Fig. 1. GRb1 reduced TBHP-induced apoptosis of H9C2 cells in a dose-dependent manner. Cells were pretreated with the indicated concentrations of GRb1 (25, 50, and 100 μM) or NAC (1 mM) for 24 h and then stimulated with TBHP (150 μM) for 2 h. The apoptosis index was determined by annexin V/PI staining. (A) Representative images of annexin V/PI staining. (B) Percentage of apoptotic H9C2 cells. (C) Viability of H9C2 cells. (D) LDH release. (E) Western blot analysis of BAX, BCL-2, and GAPDH. (F) BAX and BCL-2 expressions were normalized to that of GAPDH. Data are presented as the mean ± SD. $^{*}p < 0.05$, $^{**}p < 0.01$ vs. the TBHP group. GRb1, ginsenoside Rb1; LDH, lactate dehydrogenase; NAC, *N*-acetyl-L-cysteine; TBHP, *tert*-butyl hydroperoxide.

induce oxidative stress in H9C2 cells, resulting in the generation of large amounts of ROS; 150 μM TBHP increased ROS content in H9C2 cells to 330.8 ± 17.39% ($p < 0.01$), indicating that TBHP treatment could be used to establish an oxidative stress model group in subsequent experiments *in vitro* (Fig. 2A–B). Besides, our results indicated that GRb1 effectively inhibited ROS generation. GSH scavenges ROS in intracellular antioxidant systems [29]. Our findings showed that GRb1 dose-dependently abolished the TBHP-induced decrease in GSH level (Fig. 2C). Considering that GR activity is crucial for GSH maintenance, GR activity was investigated to assess the effect of GRb1. As shown in Fig. 2D, GRb1 protected GR activity from TBHP in a dose-dependent manner, which explains the GSH content-maintaining and ROS-reducing effects of GRb1 during TBHP treatment, as well as further inhibition of apoptosis.

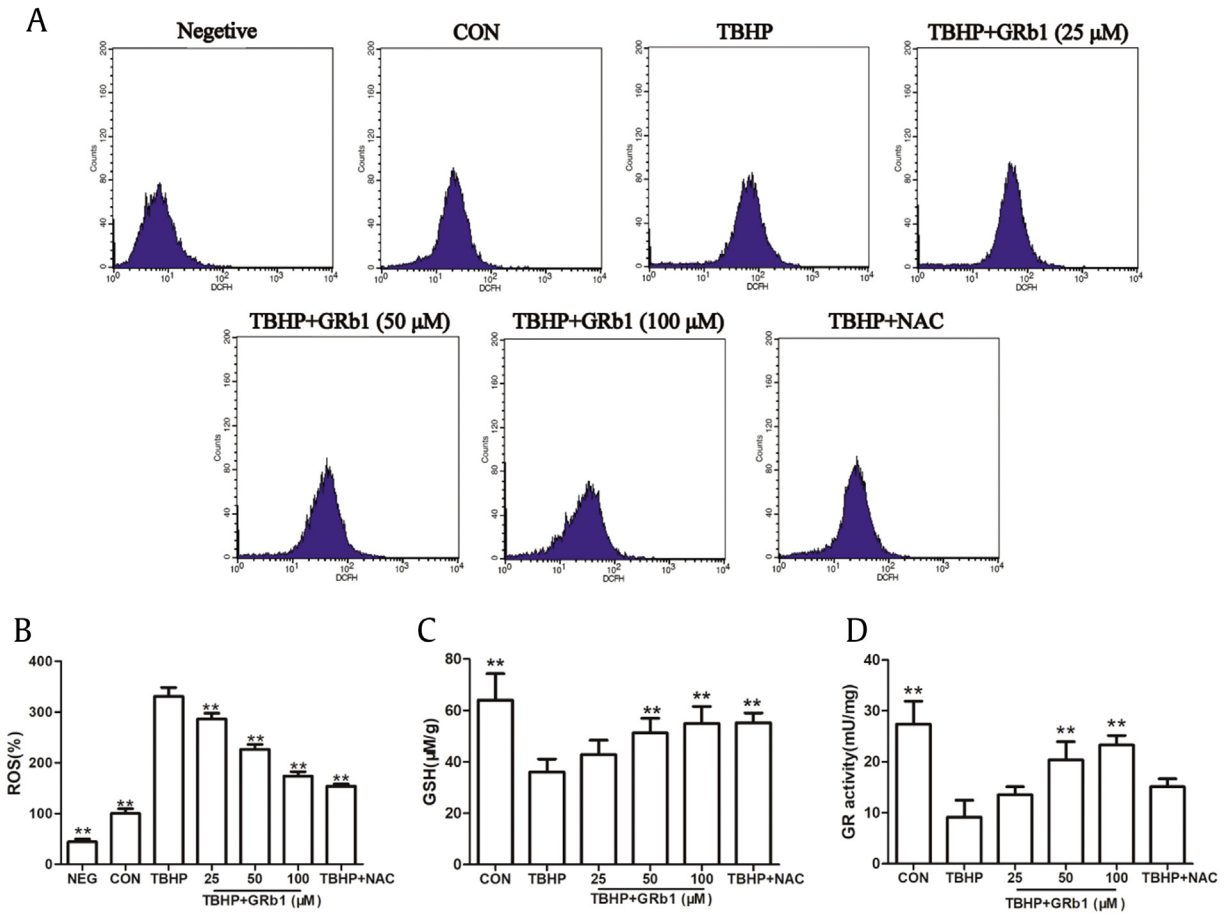

Fig. 2. GRb1 alleviated TBHP-induced oxidative stress in H9C2 cells in a dose-dependent manner. Cells were pretreated with the indicated concentrations of GRb1 (25, 50, and 100 μM) or NAC (1 mM) for 24 h and then stimulated with TBHP (150 μM) for 2 h. ROS and GSH levels and GR activity were determined. (A) ROS detection by flow cytometry. (B) ROS concentration in H9C2 cells. (C) Protection of GSH level by GRb1 in a dose-dependent manner(D) Protection of GR activity by GRb1 in a dose-dependent manner. $^{*}p < 0.05$, $^{**}p < 0.01$ vs. the TBHP group. GR, glutathione reductase; GRb1, ginsenoside Rb1; GSH, glutathione; NAC, *N*-acetyl-L-cysteine; ROS, reactive oxygen species; TBHP, *tert*-butyl hydroperoxide.

Physiologically, there are two systems, enzymatic and nonenzymatic, that allow cells to resist ROS-induced damage [30]. However, ROS generation can be excessive under pathological conditions and can overwhelm the defense systems. In the present study, we found that NAC decreased ROS level, which was consistent with data from previous studies [23,31]; moreover, it significantly increased GSH level. In addition, GRb1 served as an antioxidant and significantly reduced ROS level, which was increased by TBHP. This effect was due to the upregulation of GSH level and GR activity by GRb1. Although NAC and GRb1 showed similar effects on GSH levels, the effect of GRb1 on GR activity was found to be higher than that of NAC. It has been reported that NAC contains an SH group and is deacetylated in cells to generate cysteine, which is an important nonenzymatic antioxidant and a substrate for GSH synthesis. Consequently, a high cysteine level results in the increased intracellular production of GSH and in reduced ROS levels. Thus, NAC increased GSH level but not necessarily by enhancing GR activity. These findings show that GRb1 possibly increases GR activity to exert its antiapoptotic and antioxidant effects.

3.3. Molecular docking and molecular dynamics of GRb1 and GR

To verify whether GRb1 exerts a protective effect on TBHP-treated H9C2 cells mainly by activating GR activity, molecular docking between GRb1 and GR was performed. The optimal binding conformation of the GRb1− GR complex is shown in Fig. 3A. From the results, GRb1 interacted with Arg-347, Arg-37, Pro-368, Thr-339, Val-370, and Lys-66 residues in GR via van der Waals forces. Additionally, the binding energy between GR and GRb1 was found to be −6.426 kcal/mol. Next, molecular dynamics simulation was performed to verify the molecular docking results. The best conformation of the GRb1−GR complex, obtained from the docking analysis, was taken as the initial conformation for the molecular dynamics simulation. Surface visualization models of GRb1−GR complexes were monitored at 0–100 ns during the molecular dynamics experiment. As shown in Fig. 3B, at the beginning of the molecular dynamics simulations, GRb1 was docked into the deep center of the ligand (inhibitor)-binding site; however, it moved to the edge of the binding site after 100 ns of simulation. The heavy-atom root mean-square deviation (RMSD) track of the GR−GRb1 complex (Fig. 3C, red line) increased during the first 5 ns and fluctuated around 2.5 Å at 5–28 ns. Thereafter, RMSD increased and fluctuated around 2.9 Å at 28–100 ns. The heavy-atom RMSD track of the unbound GR fluctuated around 2.8 Å at 5–100 ns (Fig. 3C, blue line). In Fig. 3D, the thermodynamic stabilities of the GR−GRb1 complex and free-state GR were determined based on the potential energy fluctuations. The track of potential energy of the GR−GRb1 complex was found to be higher than that of the unbound GR. These results suggested that the binding between GR and GRb1 is stable. Molecular docking

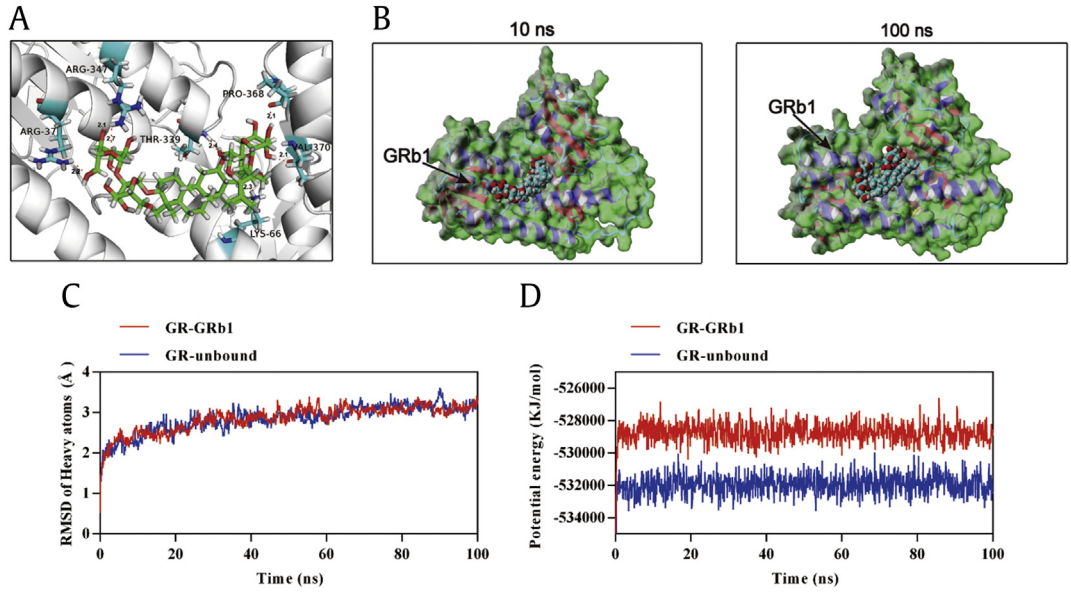

Fig. 3. Molecular docking and molecular dynamics simulations of the interaction between GRb1 and GR. (A) Crystal structure of GRb1 (CID: 9898279) in a complex with GR (PDB ID: 1GRE). GRb1 is shown in green. Hydrogen bonds are indicated by blue lines. (B) Crystal structures of the GR–GRb1 complexes at 0 and 100 ns. (C) Plots of RMSDs of the heavy atoms of unbound GR (blue) and GR–GRb1 complex (red). (D) Potential energy profiles of unbound GR (blue) and GR–GRb1 complex (red) during the 100-ns molecular dynamics simulations.

and molecular dynamic simulations are well-known computational techniques that are currently used in pharmacology [32]. In the present study, the two methods were used to predict the direct interaction between GR and GRb1, as well as to observe the physical movements of atoms and molecules in the GR–GRb1 complex. The results suggested that GRb1 could strongly bind to GR and form a favorable conformation. Moreover, the results indicate that GRb1 can exert a cardioprotective effect by stimulating GR activity.

3.4. GRb1 directly activates recombinant GR and increases basal GR activity without regulating GR expression

Based on the findings of the computational prediction study, we evaluated the influence of GRb1 on the basal activity and expression of GR. As shown in Fig. 4A, GRb1 enhanced the basal activity of GR in a dose-dependent manner. As expected, the amount of GSH was also increased dose-dependently by GRb1 (Fig. 4B). We also investigated whether GRb1 increased GR activity by upregulating

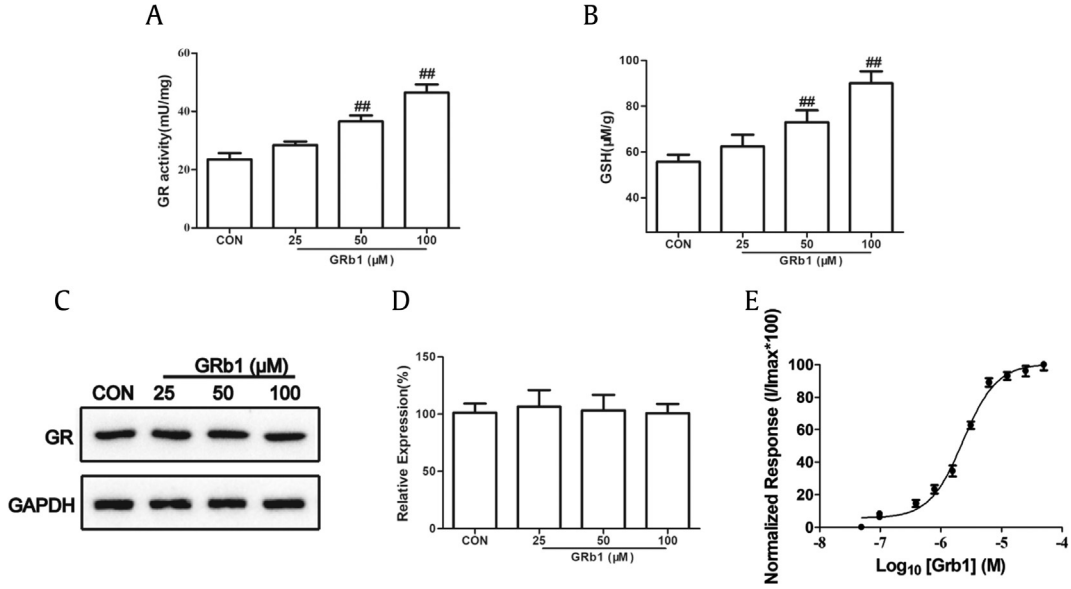

Fig. 4. GRb1 directly activated the recombinant human GR protein and increased the basal GR activity and GSH level without upregulating the GR expression in H9C2 cells. H9C2 cells were pretreated with the indicated concentrations of GRb1 (25, 50, and 100 μM) for 24 h. The basic GR activity and GSH level were determined, and western blot analysis was used to evaluate GR expression. (A) GRb1 increased the basic GR activity in a dose-dependent manner. (B) GRb1 increased GSH level in a dose-dependent manner. (C) GRb1 showed no effect on GR expression. (D) Relative expression of GR. (E) Normalized response curve of the reaction between GRb1 and recombinant human GR protein. #$p < 0.05$, ##$p < 0.01$ vs. the CON group. CON, control; GR, glutathione reductase; GRb1, ginsenoside Rb1; GSH, glutathione.

the GR protein expression. Interestingly, as shown in Fig. 4C and D, GRb1 treatment did not alter GR expression. Currently, there are no reports on GR agonists; therefore, a recombinant human GR protein was used in this study. Consistent with the results obtained with H9C2 cells, we found that GRb1 could significantly directly enhance the activity of the recombinant human GR protein. The curve shown in Fig. 4E suggested that GRb1 improved GR activity dose-dependently within a certain concentration range. The EC_{50} and $\log_{10}$-transformed EC_{50} values were found to be 2.317 and -5.635 ± 0.039 μM, respectively. The data obtained indicate that GRb1 is a potential GR agonist. Herbal antioxidants are popular, owing to their lower toxicities compared with those of synthetic molecules [33,34]. GR has been known for a long time to prevent oxidative stress and apoptosis; however, to the best of our knowledge, this is the first report on a GR agonist and its biological function. Furthermore, this is the first study to demonstrate that GRb1 enhances the basal GR activity in cells and directly activates a recombinant human GR protein. We believe that GRb1can serve as a natural GR agonist to protect against oxidative stress and apoptosis.

3.5. Inhibition of GR activity attenuated the protective effect of GRb1 against TBHP-induced oxidative stress

To further evaluate the involvement of GR in the cardioprotective effects of GRb1, H9C2 cells were treated with BCNU, an inhibitor of GR activity [35]. Our data demonstrated that BCNU could inhibit basal GR activity in the cells without changing GR expression (data not shown). Additionally, the GRb1-induced increase in GR activity was partly inhibited by BCNU, depending, however, on GSH level (Fig. 5A–D). Consistently, BCNU mostly abolished the protective effect of GRb1 against ROS generation (Fig. 5E and F). These results indicated that the antioxidative effects of GRb1 were mostly counteracted by BCNU, which implies that GRb1 exerts its antioxidative effects mainly via GR activation.

3.6. Inhibition of GR activity attenuated the protective effect of GRb1 against TBHP-induced apoptosis

To investigate whether GR activity was involved in the anti-apoptotic effect of GRb1, annexin V/PI, MTT, and LDH release assays, as well as Western blot analysis, were performed in cells co-treated with BCNU. Based on the results of annexin V/PI staining (Fig. 6A and B), the apoptosis rate of the GRb1-treated cells increased from 26.8% to 50.2% in the presence of BCNU. This indicated that the protective effect of GRb1 against TBHP-induced apoptosis was partly reduced by BCNU. Additionally, cell viability decreased from 83.8% to 58.6% (Fig. 6C) in the presence of BCNU. Moreover, the BAX/BCL-2 ratio was reversed in the GRb1-treated cells when BCNU was added to the culture medium. The results shown in Fig. 6 suggested that the antiapoptotic effect of GRb1 was due, at least in part, to the activation of GR.

The experiments with BCNU, described in Sections 3.5 and 3.6, further supported the role of GR in the antioxidative and anti-apoptotic effects of GRb1. In the present study, we obtained novel evidence suggesting that GRb1 protects against the TBHP-induced oxidative stress and apoptosis by increasing GR activity. These results provide a significant basis for further studies addressing the cardioprotective effects of GRb1 against cardiomyocyte injury. More importantly, the stimulatory effect of GRb1 on GR activity indicated that GRb1 acts as a GR agonist, which implies that GRb1 can serve as a positive control in future studies on GR.

Taken together, a series of experiments was designed in this study to elucidate the underlying mechanism by which GRb1

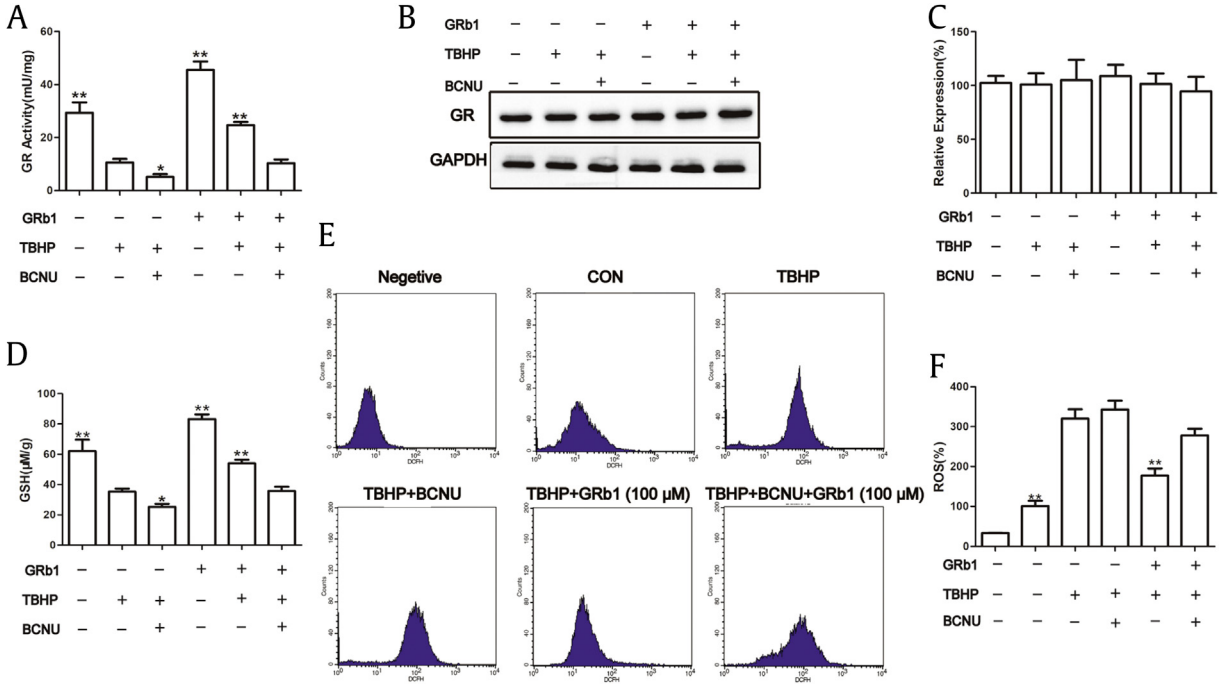

Fig. 5. Inhibition of GR activity by BCNU partly inhibited the antioxidative effects of GRb1. H9C2 cells were pretreated with or without the GR inhibitor BCNU (50 μM) for 2 h and with 100 μM GRb1 for 24 h. Then, the cells were incubated with or without TBHP (150 μM) for 2 h. (A) BCNU abolished the protective effect of GRb1 on GR activity. (B) BCNU and GRb1 showed no effect on GR expression. (C) Relative GR expression with BCNU and GRb1 treatment. (D) BCNU abolished the protective effect of GRb1 on GSH level. (E) ROS detection by flow cytometry. (F) ROS concentration in H9C2 cells (the first group was the negative group and the second group was control group). $^{*}p < 0.05$, $^{**}p < 0.01$ vs. the TBHP group. BCNU, 1,3-*bis*-(2-chloroethyl)-1-nitrosourea; GR, glutathione reductase; GRb1, ginsenoside Rb1; GSH, glutathione; ROS, reactive oxygen species; TBHP, *tert*-butyl hydroperoxide.

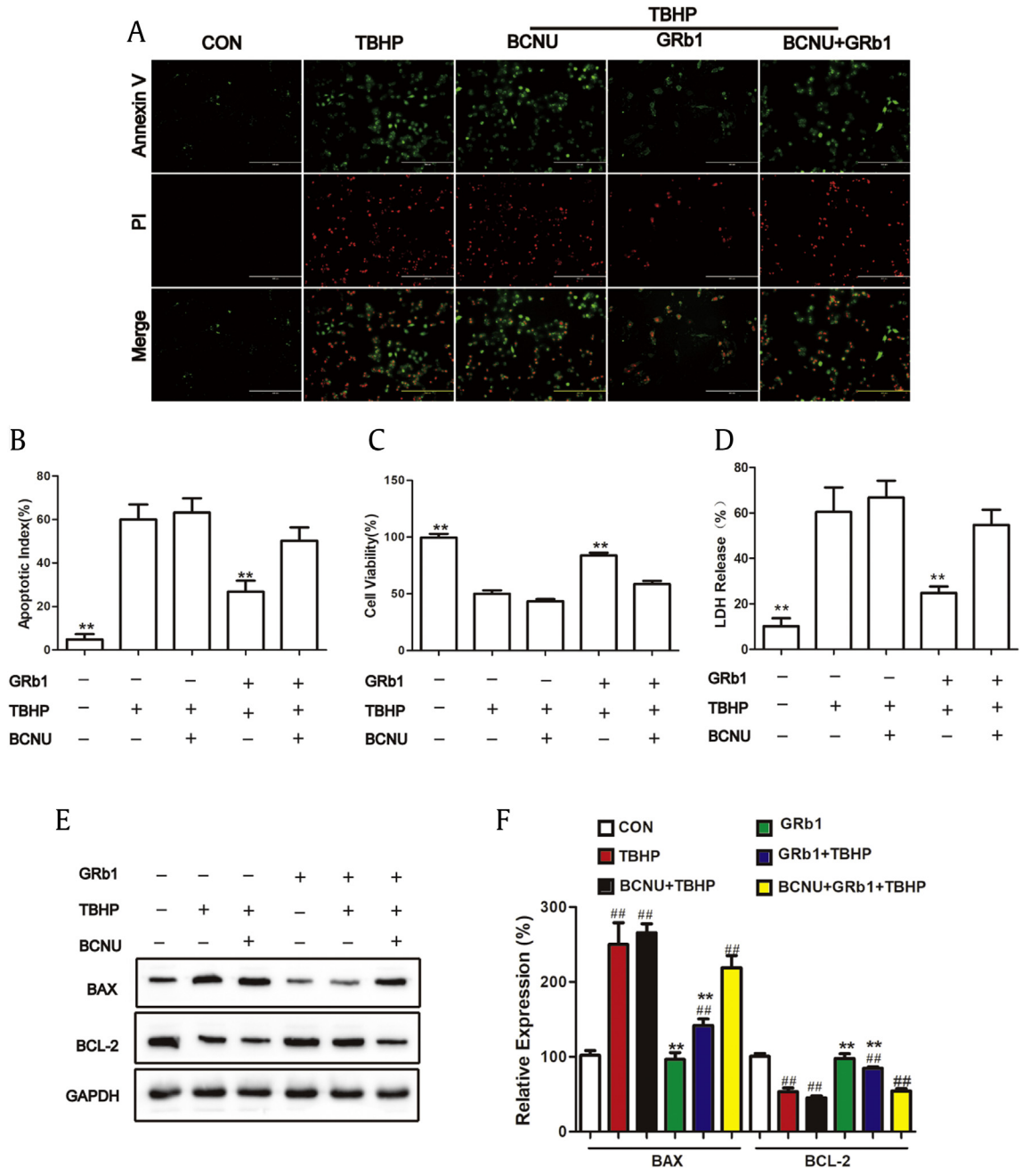

Fig. 6. Inhibition of GR activity by BCNU partly inhibited the antiapoptotic effect of GRb1. H9C2 cells were pretreated with or without the GR inhibitor BCNU and with 100 μM GRb1 for 24 h. Then, the cells were incubated with or without TBHP (150 μM) for 2 h. (A) Representative images of annexin V/PI staining. (B) Percentage of apoptotic H9C2 cells, as determined by annexin V/PI staining. (C) Viability of H9C2 cells, as determined by the MTT assay. (D) LDH release was affected by BCNU and GRb1. (E) Representative western blots of BAX, BCL-2, and GAPDH expression. (F) BAX and BCL-2 levels were normalized to that of GAPDH, and their ratios were calculated. Data are presented as the mean ± SD. $^{*}p < 0.05$, $^{**}p < 0.01$ vs. the TBHP group. $\#p < 0.05$, $\#\#p < 0.01$ vs. the CON group. BCNU, 1,3-*bis*-(2-chloroethyl)-1-nitrosourea; CON, control; GR, glutathione reductase; GRb1, ginsenoside Rb1; GSH, glutathione; PI, propidium iodide; ROS, reactive oxygen species; TBHP, *tert*-butyl hydroperoxide; SD, standard deviation; MTT, 3-(4,5-dimethylthiazol-2-yl)-2,5-diphenyltetrazolium bromide.

inhibits oxidative stress–induced myocardial apoptosis. The main findings of our study are as follows: (i) GRb1 could be constitutively docked into GR, and the interaction between GR and GRb1 was stable; (ii) GRb1 enhanced GR activity in H9C2 cells under basal and oxidative stress conditions and activated a recombinant human GR protein in a dose-dependent manner; and (iii) the cardio protective effects of GRb1 depended on GR activation.

4. Conclusions

This study was conducted to elucidate the mechanisms by which GRb1 inhibits the oxidative stress–induced apoptosis of cardiomyocytes. Our results showed that the antioxidative and antiapoptotic effects of GRb1 were counteracted by BCNU, indicating that GR activity plays a crucial role in the protective effects of GRb1. Furthermore, GRb1 enhanced the basal GR activity and GSH

levels, which led to a reduction in ROS levels. The compound also enhanced GR activity in H9C2 cells under oxidative stress conditions. We also found that GRb1 could be constitutively docked into GR in a stable manner. Overall, the findings show that GRb1 is a potential natural agonist of GR and can protect against oxidative stress–related CVDs.

Conflicts of interest

All authors have no conflicts of interest to declare.

Acknowledgments

This work was supported by grants from National Natural Science Foundation of China (81673805, 81373575, and 8177410), Science and Technology Planning Project of Guangdong Province (2014A020221013 and 2014A020221059), Traditional Chinese Medicine Bureau of Guangdong Province (20161260), and Climbing Program Special Funds of Guangdong Province (pdjh2017a0094).

References

[1] Wu D, Hu Q, Liu X, Pan L, Xiong Q, Zhu YZ. Hydrogen sulfide protects against apoptosis under oxidative stress through SIRT1 pathway in H9c2 cardiomyocytes. Nitric Oxide : Biol Chem 2015;46:204–12.
[2] Shafaroodi H, Hashemi M, Sharif ZN, Moezi L, Janahmadi Z, Dehpour AR. The possible role of nitric oxide and oxidative stress in the enhanced apoptosis of cardiac cells in cirrhotic rats. Acta Med Iran 2017;55(1):29–34.
[3] Wang X, Liu X, Zhou Q, Du J, Zhang T, Lu Y, Su S. Ginsenoside Rb1 reduces isoproterenol-induced cardiomyocytes apoptosis in vitro and in vivo. Evidence-based complementary and alternative medicine, vol. 2013. eCAM; 2013.
[4] Song JH, Shin MS, Hwang GS, Oh ST, Hwang JJ, Kang KS. Chebulinic acid attenuates glutamate-induced HT22 cell death by inhibiting oxidative stress, calcium influx and MAPKs phosphorylation. Bioorg Med Chem Lett 2017.
[5] Potts MB, Vaughn AE, McDonough H, Patterson C, Deshmukh M. Reduced Apaf-1 levels in cardiomyocytes engage strict regulation of apoptosis by endogenous XIAP. J Cell Biol 2005;171(6):925–30.
[6] Sekhar RV, Patel SG, Guthikonda AP, Reid M, Balasubramanyam A, Taffet GE, Jahoor F. Deficient synthesis of glutathione underlies oxidative stress in aging and can be corrected by dietary cysteine and glycine supplementation. Am J Clin Nutr 2011;94(3):847–53.
[7] Bolfa P, Vidrighinescu R, Petruta A, Dezmirean D, Stan L, Vlase L, Damian G, Catoi C, Filip A, Clichici S. Photoprotective effects of Romanian propolis on skin of mice exposed to UVB irradiation. Food Chem Toxicol: Int J Pub Br Ind Biol Res Assoc 2013;62:329–42.
[8] Kudugunti SK, Vad NM, Ekogbo E, Moridani MY. Efficacy of caffeic acid phenethyl ester (CAPE) in skin B16-F0 melanoma tumor bearing C57BL/6 mice. Invest N Drugs 2011;29(1):52–62.
[9] Franco R, Bortner C, Schmitz I, Cidlowski JA. Glutathione depletion regulates both extrinsic and intrinsic apoptotic signaling cascades independent from multidrug resistance protein 1. Apoptosis Int J Program Cell Death 2014;19(1):117–34.
[10] Chen C, Jiang X, Lai Y, Liu Y, Zhang Z. Resveratrol protects against arsenic trioxide-induced oxidative damage through maintenance of glutathione homeostasis and inhibition of apoptotic progression. Environ Mol Mutagen 2015;56(3):333–46.
[11] Kim SJ, Jung HJ, Hyun DH, Park EH, Kim YM, Lim CJ. Glutathione reductase plays an anti-apoptotic role against oxidative stress in human hepatoma cells. Biochimie 2010;92(8):927–32.
[12] Cereser C, Boget S, Parvaz P, Revol A. Thiram-induced cytotoxicity is accompanied by a rapid and drastic oxidation of reduced glutathione with consecutive lipid peroxidation and cell death. Toxicology 2001;163(2–3):153–62.
[13] Liu B, Zhang J, Liu W, Liu N, Fu X, Kwan H, Liu S, Liu B, Zhang S, Yu Z, et al. Calycosin inhibits oxidative stress-induced cardiomyocyte apoptosis via activating estrogen receptor-alpha/beta. Bioorg Med Chem Lett 2016;26(1):181–5.
[14] Li J, Shao ZH, Xie JT, Wang CZ, Ramachandran S, Yin J, Aung H, Li C, Qin G, Vanden Hoek T, et al. The effects of ginsenoside Rb1 on JNK in oxidative injury in cardiomyocytes. Arch Pharm Res 2012;35(7):1259–67.
[15] Zheng X, Wang S, Zou X, Jing Y, Yang R, Li S, Wang F. Ginsenoside Rb1 improves cardiac function and remodeling in heart failure. Exp Anim 2017;66(3):217–28.
[16] Cui YC, Pan CS, Yan L, Li L, Hu BH, Chang X, Liu Y, Fan J, Sun K, Li Q, et al. Ginsenoside Rb1 protects against ischemia/reperfusion-induced myocardial injury via energy metabolism regulation mediated by RhoA signaling pathway. Sci Rep 2017;7:44579.
[17] Zhu Y, Hu C, Zheng P, Miao L, Yan X, Li H, Wang Z, Gao B, Li Y. Ginsenoside Rb1 alleviates aluminum chloride-induced rat osteoblasts dysfunction. Toxicology 2016;368–369:183–8.
[18] Chen W, Wang J, Luo Y, Wang T, Li X, Li A, Li J, Liu K, Liu B. Ginsenoside Rb1 and compound K improve insulin signaling and inhibit ER stress-associated NLRP3 inflammasome activation in adipose tissue. J Ginseng Res 2016;40(4):351–8.
[19] Yu X, Ye L, Zhang H, Zhao J, Wang G, Guo C, Shang W. Ginsenoside Rb1 ameliorates liver fat accumulation by upregulating perilipin expression in adipose tissue of db/db obese mice. J Ginseng Res 2015;39(3):199–205.
[20] Li J, Shao Z, Xie JT, Wang CZ, Ramachandran S, Yin J, Aung H, Li CQ, Qin G, Vanden Hoek T, et al. The effects of ginsenoside Rb1 on JNK in oxidative injury in cardiomyocytes. Arch Pharm Res 2012;35(7):1259–67.
[21] Sardão VA, Oliveira PJ, Holy J, Oliveira CR, Wallace KB. Vital imaging of H9c2 myoblasts exposed to tert-butylhydroperoxide – characterization of morphological features of cell death. BMC Cell Biol 2007;8:11.
[22] Saha S, Sadhukhan P, Sinha K, Agarwal N, Sil PC. Mangiferin attenuates oxidative stress induced renal cell damage through activation of PI3K induced Akt and Nrf-2 mediated signaling pathways. Biochem Biophy Rep 2016;5:313–27.
[23] Chen J, Guo R, Yan H, Tian L, You Q, Li S, Huang R, Wu K. Naringin inhibits ROS-activated MAPK pathway in high glucose-induced injuries in H9c2 cardiac cells. Basic Clin Pharmacol Toxicol 2014;114(4):293–304.
[24] Chang G, Liu J, Qin S, Jiang Y, Zhang P, Yu H, Lu K, Zhang N, Cao L, Wang Y, et al. Cardioprotection by exenatide: a novel mechanism via improving mitochondrial function involving the GLP-1 receptor/cAMP/PKA pathway. Int J Mol Med 2018;41(3):1693–703.
[25] Fan CD, Sun JY, Fu XT, Hou YJ, Li Y, Yang MF, Fu XY, Sun BL. Astaxanthin attenuates homocysteine-induced cardiotoxicity in vitro and in vivo by inhibiting mitochondrial dysfunction and oxidative damage. Front Physiol 2017;8:1041.
[26] Shen H, Matsui JI, Lei D, Han L, Ohlemiller KK, Bao J. No dramatic age-related loss of hair cells and spiral ganglion neurons in Bcl-2 over-expression mice or Bax null mice. Mol Neurodegener 2010;5:28.
[27] Chen D, Xia D, Pan Z, Xu D, Zhou Y, Wu Y, Cai N, Tang Q, Wang C, Yan M, et al. Metformin protects against apoptosis and senescence in nucleus pulposus cells and ameliorates disc degeneration in vivo. Cell Death Dis 2016;7(10):e2441.
[28] Jin WS, Kong ZL, Shen ZF, Jin YZ, Zhang WK, Chen GF. Regulation of hypoxia inducible factor-1alpha expression by the alteration of redox status in HepG2 cells. J Exp Clin Cancer Res: CR 2011;30:61.
[29] Sharov VG, Sabbah HN, Shimoyama H, Goussev AV, Lesch M, Goldstein S. Evidence of cardiocyte apoptosis in myocardium of dogs with chronic heart failure. Am J Pathol 1996;148(1):141–9.
[30] Chen XL, Kunsch C. Induction of cytoprotective genes through Nrf2/antioxidant response element pathway: a new therapeutic approach for the treatment of inflammatory diseases. Curr Pharmaceut Des 2004;10(8):879–91.
[31] Wang Z, Liao SG, He Y, Li J, Zhong RF, He X, Liu Y, Xiao TT, Lan YY, Long QD, et al. Protective effects of fractions from Pseudostellaria heterophylla against cobalt chloride-induced hypoxic injury in H9c2 cell. J Ethnopharmacol 2013;147(2):540–5.
[32] Liu B, Fu XQ, Li T, Su T, Guo H, Zhu PL, Tse AK, Liu SM, YU ZL. Computational and experimental prediction of molecules involved in the anti-melanoma action of berberine. J Ethnopharmacol 2017;208:225–35.
[33] Bhattacharyya S, Pal PB, Sil PC. A 35 kD Phyllanthus niruri protein modulates iron mediated oxidative impairment to hepatocytes via the inhibition of ERKs, p38 MAPKs and activation of PI3k/Akt pathway. Food Chem Toxicol: Int J Pub Br Ind Biol Res Assoc 2013;56:119–30.
[34] Bhattacharyya S, Ghosh S, Sil PC. Amelioration of aspirin induced oxidative impairment and apoptotic cell death by a novel antioxidant protein molecule isolated from the herb Phyllanthus niruri. PloS One 2014;9(2):e89026.
[35] Chiu PY, Ko KM. Schisandrin B-induced increase in cellular glutathione level and protection against oxidant injury are mediated by the enhancement of glutathione synthesis and regeneration in AML12 and H9c2 cells. BioFactors (Oxford, England) 2006;26(4):221–30.